Biosensors and Bioelectronics 26 (2011) 3072–3076

Contents lists available at ScienceDirect

Biosensors and Bioelectronics

journal homepage: www.elsevier.com/locate/bios

Short communication

Development of a label-free impedance biosensor for detection of antibody–antigen interactions based on a novel conductive linker

Ching-Sung Chen[a], Ku-Ning Chang[a], Ying-Hua Chen[a], Chih-Kung Lee[a,b,c,*], Bryan Yong-Jay Lee[d], Adam Shih-Yuan Lee[e]

[a] Institute of Applied Mechanics, National Taiwan University, Taipei, Taiwan
[b] Engineering Science & Ocean Engineering, National Taiwan University, Taipei, Taiwan
[c] Institute for Information Industry, Taipei, Taiwan
[d] Chemical & Materials Engineering, National Central University, Chungli, Taiwan
[e] Department of Chemistry, Tamkang University, Tamsui, Taiwan

ARTICLE INFO

Article history:
Received 8 September 2010
Received in revised form
28 November 2010
Accepted 29 November 2010
Available online 7 December 2010

Keywords:
Impedance
Label-free
Conductive linker
S100
Point-of-care

ABSTRACT

We developed a label-free impedance biosensor based on an innovative conductive linker for detecting antibody–antigen interactions. As the often used conventional long chain thiol is a poor conductor, it is not a suitable material for use in a faradaic biosensor. In this study, we adopted a thiophene-based conductive bio-linker to form a self-assembled monolayer and to immobilize the bio-molecules. We used cyclic voltammetry and impedance spectroscopy to verify the enhanced conductivity properties. Results showed that the electron transfer resistance of this new conductive linker was 3 orders of a magnitude lower than for a case using a conventional long chain thiol linker. With the decreased impedance (i.e. increased faradaic current), we can obtain a higher signal/noise ratio such that the detection limit is improved. Using fluorescence microscopy, we verified that our new conductive linker has a protein immobilization capability similar to a conventional long chain thiol linker. Also, using S100 proteins, we verified the protein interaction detection capability of our system. Our obtained results showed a linear dynamic range from 10 ng/ml to 10 μg/ml and a detection limit of 10 ng/ml. With our new conductive linker, an electrochemical impedance biosensor shows great potential to be used for point-of-care applications.

1. Introduction

Over the past two decades, a variety of devices have been developed for the detection of bio-molecular interactions. Those devices have consisted of *optical* (Beusink et al., 2008; Cross et al., 2004; Cross et al., 2003; Cui et al., 2003; Lin et al., 2006a,b; Lundstrom, 1994; Swann et al., 2004), *piezoelectric* (Ayela et al., 2007; Su et al., 2005), *mechanical* (Huber et al., 2006; Tian et al., 2005) and *electrochemical* methods (Daniels and Pourmand, 2007; Darain et al., 2004; Escamilla-Gomez et al., 2009; Grieshaber et al., 2008; Katz and Willner, 2003; Komarova et al., 2010; Radi et al., 2009; Thevenot et al., 2001). Of the various types of biosensors, an optical method is thought to be the most sensitive. However the drawbacks of these types of biosensors are their large size and high cost, and the difficulty with optical alignment which has limited its adoption as a point-of-care device. In contrast, an electrochemical method such as electrochemical impedance spectroscopy (EIS) has the advantages of low cost, low power consumption and ease of miniaturization. Due to these benefits, an electrochemical biosensor is much more suitable for applications where small size and cost is crucial, such as point-of-care diagnostics (Daniels and Pourmand, 2007).

Impedance biosensors can be divided into two groups: non-faradaic and faradaic. A non-faradaic biosensor, also called a capacitive biosensor, detects bio-molecular interactions by measuring the non-faradaic current or capacitance change. The capacitance difference comes from the changes in the dielectric constant, charge distribution, dimension and shape when bio-molecular interaction occurs. The major drawback of a capacitive biosensor is that the self-assembled monolayer (SAM) and the bio-recognition layer are more crucial than in a faradaic biosensor as ions can move through the defect area and cause a short circuit, leading to a decrease or absence of the signal if these layers are not well insulated (Berggren et al., 2001). In contrast, a faradaic biosensor measures the change in the faradaic current caused from the oxidation/reduction of redox-active species. The two main factors which affect faradaic current are steric hindrance and electrostatic

* Corresponding author at: Institute of Applied Mechanics, National Taiwan University, Taipei, Taiwan. Tel.: +886 2 3366 5646; fax: +886 2 3366 5638.
E-mail addresses: cklee@ntumems.net, cklee@mems.iam.ntu.edu.tw (C.-K. Lee).

0956-5663/$ – see front matter © 2010 Elsevier B.V. All rights reserved.
doi:10.1016/j.bios.2010.11.051

repulsion (Chen et al., 2008; Daniels and Pourmand, 2007; de-los-Santos-Alvarez et al., 2007; Ding et al., 2005; Long et al., 2003). This means that the greater interaction between the biological recognition element and the analyte, the larger the steric hindrance which then results in a change in the faradaic current and impedance. In addition, the increased free charges of the bio-molecule, the larger the electrostatic repulsion between the bio-molecule and the redox-active species that can change the impedance dramatically. This characteristic gives a faradaic biosensor the ability to detect both large bio-molecules such as cells (Maalouf et al., 2007; Nandakumar et al., 2008; Ruan et al., 2002) and small bio-molecules such as DNA (Bardea et al., 1999; Long et al., 2003; Vagin et al., 2002). Since impedance changes with analyte concentration, we can estimate the analyte concentration by measuring the impedance difference.

As it is not easy for bio-molecules to bind directly to a substrate such as Au, thiol or silane is typically used as the linker to immobilize a biological recognition element. For a Au substrate, a long chain thiol linker is preferred as it can bind to the Au surface much more effectively than a short chain thiol linker (Ding et al., 2005; La Belle et al., 2007). However, a conventional long chain thiol such as 12-mercaptododecanoic acid is nonconductive and acts as a blocking effect for the redox-active pair (Berggren et al., 2001; Berggren and Johansson, 1997; Mirsky et al., 1997). The blocking effect results in a high impedance which if the impedance analyzer is not sensitive enough, the change from the protein interactions cannot be detected. For example, if the impedance after a long chain thiol linker modification was 1.07 MΩ in our system and the applied voltage was 5 mV, the resulting current obtained would be 4.67 nA, which is in the same scale of noise generated from electronic elements. Therefore, a conventional long chain thiol is not a suitable linker for a faradaic biosensor. To overcome this limitation, we adopted a thiophene-based conductive bio-linker as an alternative to the conventional long chain thiol to immobilize bio-molecules. The most significant difference between this new conductive bio-linker and long chain thiol is that the S2TA contains two thiophenes whose π orbit enhances the electron transfer ability. In addition, the dihedral angle between the two thiophenes is nearly zero such that the electron can easily transfer from one thiophene to the other. Because of this conductive property, the derivatives of the thiophene can be used as the conducting material for developing an organic field effect transistor (OFET) (Collet et al., 2000). Although benzene also contains a π orbit, the dihedral angle is much larger than for thiophene which leads to a decrease in the electron transfer ability. It is based on these advantages that we chose a thiophene-based bio-linker for this study. In this study, we used fluorescence microscopy to verify the protein immobilization capability of our new conductive bio-linker. We used S100 proteins, which are a biomarker for cardiomyopathies (Marenholz et al., 2004), to demonstrate the protein interactions measurement in our system. To test the activity and specificity of antiS100, an enzyme-linked immunosorbent assay (ELISA) experiment was also performed. To our knowledge, this is the first time this kind of linker has been used to form a SAM and to immobilize a biological recognition element using a faradaic biosensor.

2. Experimental details

2.1. Chemicals and solutions

The conductive linker, 5′-(mercaptomethyl)-2,2′-bithiophene-5-carbaldehyde (S2TA), was synthesized and the solution was prepared with CH_2Cl_2 at a concentration of 5 mM. The bisthiophenyl alcohol was converted to its corresponding acetylthiol by a Mitsunobu reaction which then underwent hydrolysis to have thiol functionality. The bisthiophenyl thiol compound was treated with $POCl_3$ and N,N-dimethyl fomamide (DMF) to generate the expected S2TA product (refer to Supplementary data). The 12-Mercaptododecanoic acid ($HS(CH_2)_{11}COOH$, Aldrich), abbreviated as 12-MCA, was used without further purification. The 12-MCA solution was prepared by dissolving in 95% ethanol. The concentration was 20 mM. The phosphate buffered saline (PBS) solution was supplied by UR and used for the preparation of the mouse monoclonal antiS100 (abcam), S100 protein (Sigma) and horseradish peroxidase (HRP) conjugated mouse IgG secondary antibody (abcam) solutions. The electrolyte for the electrochemical experiment was a 1× PBS, pH 7.2 with 1 mM $K_3Fe(CN)_6/K_4Fe(CN)_6$ (Sigma–Aldrich) mixing solution and was prepared immediately before usage. The *N*-Hydroxysuccinimide (NHS) and N-Ethyl-N′-(3-dimethylaminopropyl) carbodiimide hydrochloride (EDC) were obtained from Fluka and Sigma–Aldrich, respectively. The ethanolamine hydrochloride (ETA-HCl) and glycine were from Sigma–Aldrich and Sigma, respectively. The ELISA reagents, such as coating solution, BSA blocking, TMB peroxidase substrate, TMB stop solution and wash solution, were from KPL (USA). All the solutions were prepared with D.I. water purified through a Milli-Q system (Millipore).

2.2. Chip preparation for fluorescence measurement

The gold-coated glass chip was first cleaned with a piranha solution for 3 min. After thoroughly rinsing with D.I. water, the chip was dried by a N_2 stream. The cleaned chip was then immersed in S2TA and 12-MCA solutions. Since a thiol linker can form an effective SAM within 6 h (Ding et al., 2005; Firagoso et al., 2008; Komura et al., 2004; Lai et al., 2006), the 12-MCA modification time was set for 6 h. For S2TA, since it is a new linker, we immersed the chip in an S2TA solution for 6 h and 12 h to see the time effect on the protein immobilization capability. After modification, the 12-MCA and S2TA modified chips were rinsed with ethanol and CH_2Cl_2 respectively and again washed with D.I. water. After drying with a N_2 stream, the 12-MCA chip was immersed in a 400 mM EDC/100 mM NHS (1:1) mixture solution for 40 min in order to activate the carboxyl group, and then modified with 5 μg/ml FITC–avidin (BioLegend) for another 40 min. The S2TA chip was modified without any further activation. For the control experiment, we also added FITC–avidin on a bare gold chip for 40 min. After immobilization of the FITC–avidin, all the items (e.g. modified 12-MCA, modified S2TA and bare chip) were all rinsed with D.I. water and dried with N_2.

2.3. Fluorescence measurement

Before starting our experiments, the fluorescent microscope (IX71, Olympus) light source was warmed up for at least 15 min. The excitation wavelength of the FITC was 488 nm and induced a light emission maximum at 520 nm. To reduce background noise, a filter (U-MWG2, Olympus) was used. The fluorescent image was captured with a CCD camera (DP30BW, Olympus) at an exposure time of 500 ms and then analyzed with ImageJ software (National Institutes of Health, USA).

2.4. ELISA measurement procedures

The S100 protein, C-reactive protein (CRP, Sigma) and human serum albumin (HAS, Sigma) were diluted with a coating solution and coated on a 96-well plate at 4 °C overnight. The 1% BSA blocking solution was added and allowed to set for 1 h before being injecting with a 2.5 μg/ml mouse monoclonal antiS100 for another hour. Then 0.4 μg/ml HRP conjugated mouse IgG secondary antibody was added and incubated for 1 h. The plate was washed 5 times with a

wash solution between each of the above steps. The TMB peroxidase substrate was added for 30 min and followed by a stop solution for 5 min. An ELISA reader (μ*Quant*, BioTek) was used for scanning the optical density (OD) of each well. For the control portion, only a TMB peroxidase substrate and stop solution were added.

2.5. Modification of a gold electrode for electrochemical measurements

The 2 mm diameter Au electrode (CH Instrument) was polished with a 0.05 μm alumina slurry and a microcloth pad and then ultrasonically cleaned in D.I. water. After drying with a stream of N_2, the electrode was immersed in the 12-MCA and S2TA solution respectively for 6 h at room temperature. Then, the 12-MCA modified electrode was rinsed with ethanol and D.I. water. The S2TA modified electrode was rinsed with CH_2Cl_2, ethanol and D.I. water. Then, both the 12-MCA and S2TA modified electrodes were dried using N_2.

2.6. Antibody immobilization for antibody–antigen interaction measurements

To immobilize the antibody, a 200 μg/ml monoclonal antiS100 was added on the S2TA modified electrode for 40 min. After rinsing with 1× PBS, a 1 M ETA-HCl at pH 8.2 was introduced for 20 min to block the unreacted aldehyde group. Different concentrations of the S100 were then prepared at 1× PBS (at pH 7.2), from 10 ng/ml to 10 μg/ml which were then added to interact with the antiS100 for 15 min. To regenerate the surface 0.1 M glycine, pH 2.5 was used.

2.7. Electrochemical measurements

All the electrochemical experiments were performed using a CHI 614D electrochemical analyzer (CH Instrument). The supporting electrolyte used was a 1× PBS containing a 1 mM $Fe(CN)_6^{3-}/Fe(CN)_6^{4-}$ (1:1) redox pair. Cyclic voltammetry (CV) and impedance measurements were carried out in a conventional three-electrode cell. An Ag/AgCl electrode and Pt wire were used as the reference and counter electrode, respectively. The potential scan range for the CV was −0.2 to +0.6 V with a scan rate at 50 mV/s. For the impedance measurement, a DC bias voltage was set at the open-circuit potential of the redox pair with a 5 mV AC amplitude in a test frequency ranging from 1 Hz to 100 kHz. The impedance data was fitted with a Randles model circuit (Katz and Willner, 2003). The parameters in the equivalent circuit such as solution resistance, R_s, electron transfer resistance, R_{et}, and double layer capacitance, C_{dl}, were determined from a fit of the model circuit to the data.

3. Results and discussion

3.1. Binding capability to bio-molecules of S2TA

This experiment was performed to verify the immobilization capability of our novel conductive linker. The bio-molecular binding capability of the linker can be estimated by measuring the fluorescence intensity change before and after binding with FITC–avidin (Sapsford and Ligler, 2004; Tedeschi et al., 2003). Table 1 shows the fluorescence intensity differences of the FITC–avidin binding. I_0 and $I_{FITC-avidin}$ represent the intensity before and after immobilization of the FITC–avidin, respectively. In our study, our sample size was based on 10 samples. For the case with a bare electrode, the intensity increased after FITC–avidin immobilization, which was 5 times larger than the standard deviation of I_0 and $I_{FITC-avidin}$. Since there was no bio-linker bound to the bare electrode, we can assume that the intensity increase is the result of the non-specific adsorption of the FITC–avidin. For the case of the S2TA at 6 h and S2TA at 12 h, the increased fluorescence intensity was nearly the same and the increased value was three times that for the bare electrode, we infer that the FITC–avidin did indeed bind to the S2TA and also that 6 h is enough time to form a S2TA SAM. Furthermore, the difference between $\Delta I_{12MCA\text{-}6\,h}$ and $\Delta I_{S2TA\text{-}6\,h}$ was 14.8 which is within the standard deviation of the measured intensity. We can therefore conclude that S2TA has a similar bio-molecular binding capability to a conventional thiol linker.

Table 1
Fluorescence measurement results (n = 10). (Note: the expression of the data is a mean value with its standard deviation).

	I_0	$I_{FITC-avidin}$	ΔI
Bare	6019.3 ± 24.7	6147.2 ± 27.9	127.9
12 MCA-6 h	5958.0 ± 21.1	6329.1 ± 27.3	371.1
S2TA-6 h	5989.2 ± 24.4	6375.1 ± 32.1	385.9
S2TA-12 h	5953.8 ± 25.7	6320.1 ± 20.4	366.3

3.2. Electrochemical characterization of 12-MCA and S2TA SAM

Cyclic voltammetry is often used to measure the blocking effect of a SAM modified on an electrode through a redox behavior of a reversible $Fe(CN)_6^{3-}/Fe(CN)_6^{4-}$ pair (Cecchet et al., 2006; Ding et al., 2005; Miller et al., 1991; Radi et al., 2009). In Fig. 1(A), a few apparent oxidation and reduction peaks at about 0.24 V and 0.18 V were found for the bare electrode. After 12-MCA modification, the peaks disappeared. This can be attributed to the blocking effect of 12-MCA on the electron transfer of the $Fe(CN)_6^{3-}/Fe(CN)_6^{4-}$ pair.

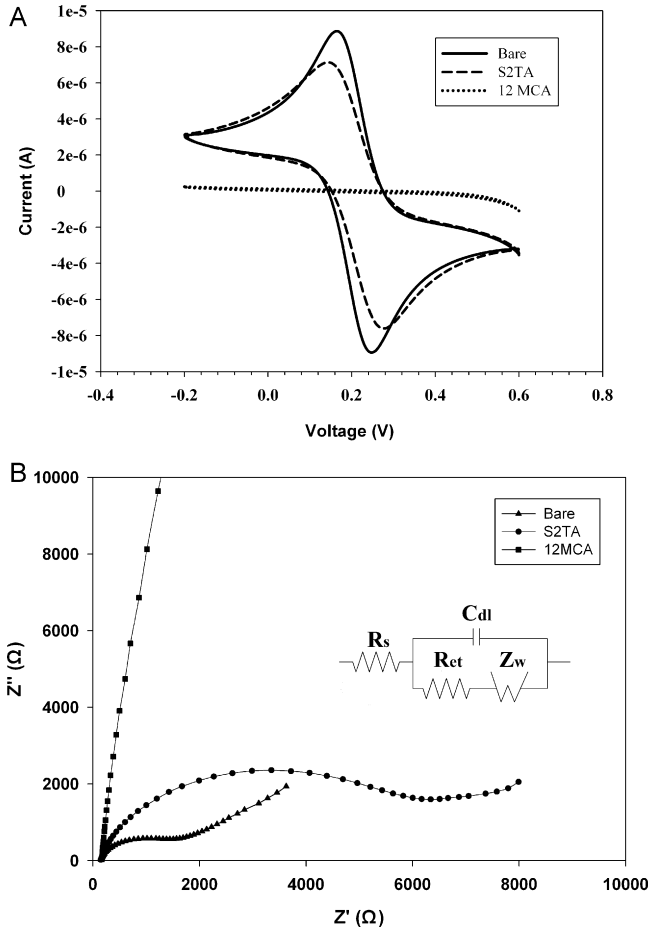

Fig. 1. Electrochemical characterization of bare, S2TA modified and 12-MCA modified electrodes: (A) cyclic voltammetry, and (B) electrochemical impedance spectroscopy. (Note: inset is the Randles model circuit).

In contrast, the redox peak was still seen for the S2TA modified electrode. This can be explained by the structure of the S2TA which contains a π orbit which enhances electron transfer. Fig. 1(B) shows the impedance data for a bare electrode, an S2TA modified electrode and a 12-MCA modified electrode. By fitting the impedance data with a Randles model circuit and analyzing with Zview software (V3.2, Scribner Associates, Inc.), the electron transfer resistance, R_{et}, was estimated to be 1.22 kΩ, 5.78 kΩ and 1.07 MΩ for the bare electrode, the S2TA modified electrode and the 12-MCA modified electrode, respectively. Results showed that the R_{et} for the S2TA modified electrode was much lower, at about three orders of magnitude, than for the case with the 12-MCA modified electrode. We also compared the current response by introducing a AC amplitude at 5 mV into our system. The current response of the S2TA and 12-MCA modified electrodes was calculated to be 870 nA and 4.67 nA, respectively. As the noise level from the general electronic element was based on a nA scale, the improved signal/noise (S/N) ratio for the S2TA versus 12MCA modified electrodes was 1000. This means that the sensitivity or de-noise design of an impedance analyzer based on the 12-MCA modified electrode need to be 1000 times better than an impedance analyzer based on an S2TA design to have the same performance. Moreover, protein interactions always further decrease the current (i.e. increase impedance) which makes detection more difficult. In contrast, for the current baseline, which was defined as a current response after SAM formation, the S2TA modified electrode was much higher than noise. In other words, biosensors based on S2TA modified electrodes will be more sensitive and possess a better detection limit. For example, if the protein interactions lead the R_{et} to increase 1 kΩ, the total R_{et} will be 1.071 MΩ for a 12-MCA modified electrode and 6.78 kΩ for an S2TA modified electrode. Although the change in R_{et} is the same, the change in the current between the two is remarkably different. For 12-MCA, the current change is less than 0.01 nA, which is 2 orders lower than noise. On the other hand, for S2TA, the change is about 130 nA, which is about 2 orders higher than noise. We can thus conclude that S2TA is much more suitable for use in a faradaic biosensor than the typically used conventional long chain thiol linker.

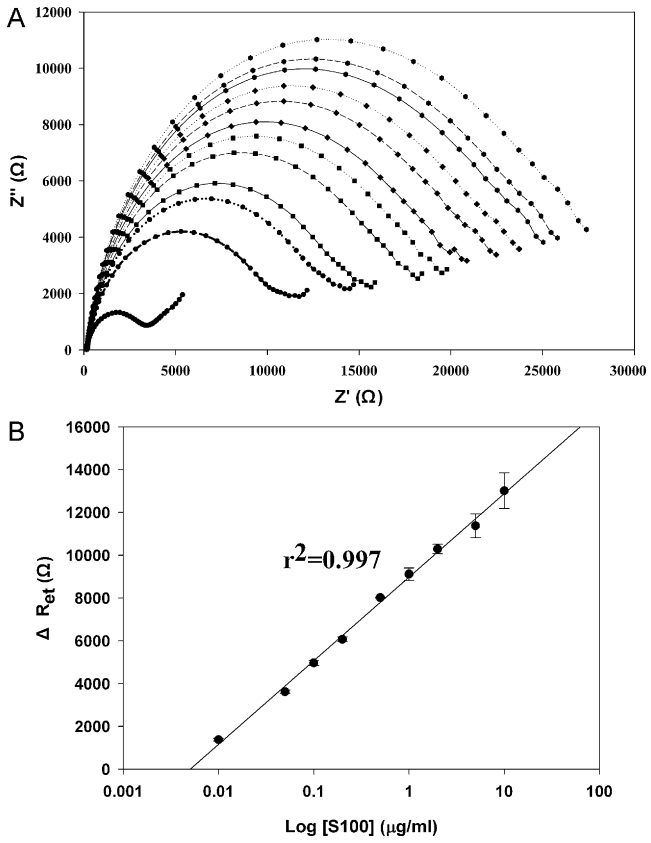

Fig. 2. Impedance data of the S2TA modified electrode in a 1× PBS solution with 1 mM $Fe(CN)_6^{3-/4-}$ after the addition of antiS100, ETA, and S100 antigen at different concentrations. (A) Nyquist plots: (a) S2TA, (b) antiS100, (c) ETA, (d) 10 ng/ml S100, (e) 50 ng/ml S100, (f) 100 ng/ml S100, (g) 200 ng/ml S100, (h) 500 ng/ml S100, (i) 1 μg/ml S100, (j) 2 μg/ml S100, (k) 5 μg/ml S100, and (l) 10 μg/ml S100. (B) Calculated R_{et} change with standard deviation (n = 3) as a function of S100 concentration ranging from 10 ng/ml to 10 μg/ml.

3.3. AntiS100 specificity test via ELISA

To test the activity of antiS100 and its specificity against S100, CRP & HSA, ELISA experiments were performed. Since CRP is also a type of cardiomyopathic biomarker and HSA is the most abundant protein in human serum, these two kinds of protein were chosen for the specificity test. Our results (shown in the Supplementary data) show that the optical density (OD) increases with the antigen concentration in the S100 case. The obtained values in our test experiments were much larger, at about 12–72 times of magnitude, than for the control experiments. In contrast, the OD values in all concentrations were at the same order as the control experiments for the CRP and HSA cases. From the results, we can deduce that the antiS100 used here can only interact with the S100 but not with the CRP or HSA.

3.4. Impedance measurement of antiS100-S100 interactions

The antiS100-S100 interactions based on the S2TA modified electrode was investigated using EIS. We repeated our experiment three times. Fig. 2(A) shows that after the addition of the antiS100, the R_{et} changed by about 8800 ± 664 Ω, which is larger than the R_{et} after S2TA modification. Since the antiS100 was nonconductive, the immobilization of antiS100 formed a steric hindrance which blocked the electron transfer of $Fe(CN)_6^{3-/4-}$. As the S100 protein interacted with the antiS100, a further increase in the R_{et} was seen. As expected, when the concentration of the S100 protein was increased, the interaction between the antiS100 and S100 also increased. This resulted in a larger steric hindrance which then caused the impedance to change more dramatically. To quantify the S100, we defined a parameter:

$$\Delta R_{et} = R_{et(S100)} - R_{et(ETA)},$$

where $R_{et(S100)}$ is the R_{et} value measured after adding the S100 protein at different concentrations, and $R_{et(ETA)}$ represents the R_{et} value before adding the S100 protein. Fig. 2(B) shows a good linear relationship between ΔR_{et} and the S100 protein which was found to be in the range between 10 ng/ml to 10 μg/ml and where the detection limit was about 10 ng/ml (0.5 nM). The calculated relative standard deviation (RSD) was about 5% at the S100 concentration from 10 ng/ml to 2 μg/ml and about 10% in the range from 5 μg/ml to 10 μg/ml. Compared to previous research using a long chain thiol as a linker (Ding et al., 2005), the detection limit in our system is much improved (82 nM VS. 0.5 nM) as the conductive linker can increase the S/N and further lower the detection limit.

4. Conclusions

We demonstrated a novel, rapid and label-free impedance-based biosensor using a new conductive linker. With the adoption of this new conductive linker, the impedance baseline after the SAM formation is in the order of kΩ, which corresponds to a μA level when the applied voltage is 5 mV. The increased S/N allows the EIS biosensor to possess a higher sensitivity and a better detection limit. We also verified that the S2TA SAM has a comparable protein immobilization capability to 12-MCA SAM. Furthermore, by using

S100 as the model protein, the obtained linear dynamic range was 10 ng/ml to 10 μg/ml and the detection limit was 10 ng/ml. Future investigations are currently in progress to improve sensor sensitivity and the detection limit. For future research, we will look towards the possibility of expanding the variety of detectable biomarkers.

Acknowledgement

The authors would like to thank the Taiwan National Science Council for its support under Project No. NSC 99-2627-E-002-002.

Appendix A. Supplementary data

Supplementary data associated with this article can be found, in the online version, at doi:10.1016/j.bios.2010.11.051.

References

Ayela, C., Roquet, F., Valera, L., Granier, C., Nicu, L., Pugniere, M., 2007. Biosens. Bioelectron. 22 (12), 3113–3119.
Bardea, A., Patolsky, F., Dagan, A., Willner, I., 1999. Chem. Commun. (1), 21–22.
Berggren, C., Bjarnason, B., Johansson, G., 2001. Electroanalysis 13 (3), 173–180.
Berggren, C., Johansson, G., 1997. Anal. Chem. 69 (18), 3651–3657.
Beusink, J.B., Lokate, A.M.C., Besselink, G.A.J., Pruijn, G.J.M., Schasfoort, R.B.M., 2008. Biosens. Bioelectron. 23 (6), 839–844.
Cecchet, F., Marcaccio, M., Margotti, M., Paolucci, F., Rapino, S., Rudolf, P., 2006. J. Phys. Chem. B 110 (5), 2241–2248.
Chen, X.J., Wang, Y.Y., Zhou, J.J., Yan, W., Li, X.H., Zhu, J.J., 2008. Anal. Chem. 80 (6), 2133–2140.
Collet, J., Tharaud, O., Chapoton, A., Vuillaume, D., 2000. Appl. Phys. Lett. 76 (14), 1941–1943.
Cross, G.H., Reeves, A., Brand, S., Swann, M.J., Peel, L.L., Freeman, N.J., Lu, J.R., 2004. J. Phys. D-Appl. Phys. 37 (1), 74–80.
Cross, G.H., Reeves, A.A., Brand, S., Popplewell, J.F., Peel, L.L., Swann, M.J., Freeman, N.J., 2003. Biosens. Bioelectron. 19 (4), 383–390.
Cui, X.Q., Pei, R.J., Wang, X.Z., Yang, F., Ma, Y., Dong, S.J., Yang, X.R., 2003. Biosens. Bioelectron. 18 (1), 59–67.
Daniels, J.S., Pourmand, N., 2007. Electroanalysis 19 (12), 1239–1257.
Darain, F., Park, D.S., Park, J.S., Shim, Y.B., 2004. Biosens. Bioelectron. 19 (10), 1245–1252.
de-los-Santos-Alvarez, N., Lobo-Castanon, M.J., Miranda-Ordieres, A.J., Tunon-Blanco, P., 2007. J. Am. Chem. Soc. 129 (13), 3808–3809.
Ding, S.J., Chang, B.W., Wu, C.C., Lai, M.F., Chang, H.C., 2005. Electrochim. Acta 50 (18), 3660–3666.
Escamilla-Gomez, V., Campuzano, S., Pedrero, M., Pingarron, J.M., 2009. Biosens. Bioelectron. 24 (11), 3365–3371.
Firagoso, A., Laboria, H., Latta, D., O'Sullivan, C.K., 2008. Anal. Chem. 80 (7), 2556–2563.
Grieshaber, D., MacKenzie, R., Voros, J., Reimhult, E., 2008. Sensors 8 (3), 1400–1458.
Huber, F., Hegner, M., Gerber, C., Guntherodt, H.J., Lang, H.P., 2006. Biosens. Bioelectron. 21 (8), 1599–1605.
Katz, E., Willner, I., 2003. Electroanalysis 15 (11), 913–947.
Komarova, E., Reber, K., Aldissi, M., Bogomolova, A., 2010. Biosens. Bioelectron. 25 (6), 1389–1394.
Komura, T., Yamaguchi, T., Shimatani, H., Okushio, R., 2004. Electrochim. Acta 49 (4), 597–606.
La Belle, J.T., Bhavsar, K., Fairchild, A., Das, A., Sweeney, J., Alford, T.L., Wang, J., Bhavanandan, V.P., Joshi, L., 2007. Biosens. Bioelectron. 23 (3), 428–431.
Lai, R.Y., Seferos, D.S., Heeger, A.J., Bazan, G.C., Plaxco, K.W., 2006. Langmuir 22 (25), 10796–10800.
Lin, S.M., Lee, C.K., Lin, Y.H., Lee, S.Y., Sheu, B.C., Tsai, J.C., Hsu, S.M., 2006a. Biosens. Bioelectron. 22 (5), 715–721.
Lin, S.M., Lee, C.K., Wang, Y.M., Huang, L.S., Lin, Y.H., Lee, S.Y., Sheu, B.C., Hsu, S.M., 2006b. Biosens. Bioelectron. 22 (2), 323–327.
Long, Y.T., Li, C.Z., Kraatz, H.B., Lee, J.S., 2003. Biophys. J. 84 (5), 3218–3225.
Lundstrom, I., 1994. Biosens. Bioelectron. 9 (9–10), 725–736.
Maalouf, R., Fournier-Wirth, C., Coste, J., Chebib, H., Saikali, Y., Vittori, O., Errachid, A., Cloarec, J.P., Martelet, C., Jaffrezic-Renault, N., 2007. Anal. Chem. 79 (13), 4879–4886.
Marenholz, I., Heizmann, C.W., Fritz, G., 2004. Biochem. Biophys. Res. Commun. 322 (4), 1111–1122.
Miller, C., Cuendet, P., Gratzel, M., 1991. J. Phys. Chem. 95 (2), 877–886.
Mirsky, V.M., Riepl, M., Wolfbeis, O.S., 1997. Biosens. Bioelectron. 12 (9–10), 977–989.
Nandakumar, V., La Belle, J.T., Reed, J., Shah, M., Cochran, D., Joshi, L., Alford, T.L., 2008. Biosens. Bioelectron. 24 (4), 1039–1042.
Radi, A.E., Munoz-Berbel, X., Lates, V., Marty, J.L., 2009. Biosens. Bioelectron. 24 (7), 1888–1892.
Ruan, C.M., Yang, L.J., Li, Y.B., 2002. Anal. Chem. 74 (18), 4814–4820.
Sapsford, K.E., Ligler, F.S., 2004. Biosens. Bioelectron. 19 (9), 1045–1055.
Su, X.D., Wu, Y.J., Knoll, W., 2005. Biosens. Bioelectron. 21 (5), 719–726.
Swann, M.J., Peel, L.L., Carrington, S., Freeman, N.J., 2004. Anal. Biochem. 329 (2), 190–198.
Tedeschi, L., Domenici, C., Ahluwalia, A., Baldini, F., Mencaglia, A., 2003. Biosens. Bioelectron. 19 (2), 85–93.
Thevenot, D.R., Toth, K., Durst, R.A., Wilson, G.S., 2001. Biosens. Bioelectron. 16 (1–2), 121–131.
Tian, F., Hansen, K.M., Ferrell, T.L., Thundat, T., 2005. Anal. Chem. 77 (6), 1601–1606.
Vagin, M.Y., Karyakin, A.A., Hianik, T., 2002. Bioelectrochemistry 56 (1–2), 91–93.